Proceedings of ITC18, 2008

1D fluid model of LHD divertor plasma and hydrogen recycling

Gakushi KAWAMURA[1)], Yukihiro TOMITA[1)], Masahiro KOBAYASHI[1)],and David TSKHAKAYA[2,3)]

[1)]*National Institute for Fusion Science, Gifu 509-5292, Japan*

[2)]*Association Euratom-ÖAW, Institute of Theoretical Physics, University of Innsbruck, Technikerstrasse 25/II, Innsbruck A-6020, Austria*

[3)]*Permanent address: Institute of Physics, Georgian Academy of Sciences, 380077 Tbilisi, Georgia*

One dimensional plasma and neutral models of the divertor plasma in Large Helical Device is presented. The plasma is described by stationary fluid equations for electron and ion. The atomic processes such as dissociation of hydrogen molecules released from the divertor plate, ionization of hydrogen atoms, charge exchange and recombination are included in equations of neutrals. This model is intended to be employed in an integrated simulation where an equilibrium of the upstream plasma and plasma-surface interactions at the divertor plate are solved in different numerical codes separately. From the computational point of view, the numerical code for the divertor plasma is developed for 1D flux tube where the boundary conditions of both ends are specified. The calculation time is less than one second and reasonably short to use in future integrated simulations. In the results, interactions between plasma and neutrals and dependence of the energy loss on the plasma density are studied. In low density case, the energy is lost through ionization and charge exchange but the total amount of the loss is small and the impurity loss is negligibly small. In high density, or high recycling case, the ionization loss and impurity cooling increases much larger than the charge exchange loss and causes the drop of the heat flux at the divertor plate.

Keywords: LHD, divertor, fluid, neutral, recycling

1 Introduction

The Large Helical Device (LHD) [1] is a heliotron / tersatron type device with helical divertors. The LHD plasma has an ergodic layer [2] outside the core plasma. The divertor plasma is connected to the ergodic layer and parallel flow along the magnetic field is dominant there. The plasma profiles such as density and temperature determine the motion and the charge state of impurities. Therefore, physical understandings of the divertor plasma and its modeling are important issues in the LHD boundary plasmas.

In this paper, we present plasma and neutral models in the divertor plasma to determine the plasma profiles from input parameters such as heat flux coming from the ergodic layer and the plasma density at the upstream boundary. The model presented here is intended to be employed in our future studies as a divertor leg model to connect the following two simulation codes; EMC3 code [2] for the ergodic layer and ERO code [3] for the plasma-surface interactions at the divertor. The former code solves fluid equations to obtain equilibrium plasma profiles in the stochastic magnetic field and the latter solves the equations of motion for impurity particles to obtain the sputtering yield, time evolution of surface conditions and impurity transport near a target plate. In order to avoid a numerical difficulty arising from the strong magnetic shear in the LHD boundary plasma and to keep the amount of the computational resources in reasonable level, we developed 1D model along the magnetic field line, i.e. a flux tube model.

The plasma fluid equations are described in Sec. 2.1. They include interaction with neutrals and impurity cooling [4–7]. The differences of our model from these models are the neutral equations discussed in Sec. 2.2, which includes atomic processes such as dissociation and ionization of hydrogen molecules and atoms. In Sec. 3, comparisons with our previous model [8] and discussion of heat flux and energy loss are given. Finally in Sec. 4, conclusions are presented.

2 Divertor plasma and neutral models

2.1 Fluid equations of plasma

We use Braginskii-type two fluid equations [9] to describe the divertor plasma. Since 1D fluid equations along the magnetic field and the method of numerical solution was reported in the previous work [8], we summarize them briefly here. We denote the plasma density, velocity, electron and ion temperatures and electrostatic potential by $n(s)$, $v(s)$, $T_e(s)$, $T_i(s)$ and $\phi(s)$, respectively. The position along the magnetic field is described by s and has zero value, $s = 0$, at the upstream boundary and the connection length, $s = l_c$, at the entrance of the magnetic presheath [10]. The four conservation equations of density, momentum and temperatures and Ohm's law, or electron momentum conservation, are given by

$$\frac{dnv}{ds} = S_n, \qquad (1)$$

author's e-mail: kawamura.gakushi@nifs.ac.jp

$$\frac{d}{ds}\left[m_{\rm i}nv^2 + n\left(T_{\rm e}+T_{\rm i}\right)\right] = S_{\rm p}, \quad (2)$$

$$\frac{d}{ds}\left[\frac{5}{2}nvT_{\rm e} - \kappa_{\rm e0}T_{\rm e}^{5/2}\frac{dT_{\rm e}}{ds}\right] = env\frac{d\phi}{ds} - \frac{3m_{\rm e}n}{m_{\rm i}}\nu_{\rm eq}(T_{\rm e}-T_{\rm i}) - Lr_{\rm imp}n^2 + S_{\rm Ee}, \quad (3)$$

$$\frac{d}{ds}\left[\frac{m_{\rm i}nv^3}{2} + \frac{5nvT_{\rm i}}{2} - \kappa_{\rm i0}T_{\rm i}^{5/2}\frac{dT_{\rm i}}{ds}\right] = -env\frac{d\phi}{ds} + \frac{3m_{\rm e}n}{m_{\rm i}}\nu_{\rm eq}(T_{\rm e}-T_{\rm i}) + S_{\rm Ei}, \quad (4)$$

$$\frac{1}{n}\frac{dnT_{\rm e}}{ds} + 0.71\frac{dT_{\rm e}}{ds} - e\frac{d\phi}{ds} = 0 \quad (5)$$

where the electron and ion mass, carbon impurity ratio, the heat conduction coefficients and temperature equilibration coefficient were denoted by $m_{\rm e}$, $m_{\rm i}$, $r_{\rm imp}$, $\kappa_{\rm i0} = 1.2\times10^{69}$ [W/mJ$^{7/2}$], $\kappa_{\rm e0} = 5.0\times10^{67}$ [W/mJ$^{7/2}$] and $\nu_{\rm eq} = 6.9\times10^{17}nT_{\rm e}^{3/2}$ [11]. The source terms associated with neutrals in the right-hand side, i.e. $S_{\rm n}$, $S_{\rm p}$, $S_{\rm Ee}$ and $S_{\rm Ei}$, are discussed later in Sec. 2.2. The following conditions and relations are assumed in these equations; i) the temperature anisotropy time is negligibly short compared with the particle dwell time, i.e. $T_\perp = T_\parallel = T$, ii) ambipoler flow, i.e. $v_{\rm e} = v_{\rm i} = v$, iii) quasineutral condition, i.e. $n_{\rm e} = n_{\rm i} = n$.

In this paper, we use variables with subscripts '0' and '1' to indicate boundary values at $s = 0$ and $l_{\rm c}$, respectively. The plasma equations, Eqs. (1) – (5), are integrated numerically from the wall to the upstream boundary. Since our model is intended to be employed to connect different simulation codes at $s = 0$ and $l_{\rm c}$, the plasma density and heat flux at the upstream boundary are implemented as free parameters. The integral of the plasma equations, however, requires boundary values at $s = l_{\rm c}$ as initial values. Therefore we utilize the Newton's method to determine the initial values satisfying the density and heat flux at $s = 0$ and the following four conditions; i) equality of the Bohm criterion at $s = l_{\rm c}$, i.e. $v_1 = c_{\rm s} \equiv \sqrt{(T_{\rm e1}+T_{\rm i1})/m_{\rm i}}$, ii) potential $\phi_1 = 0$, iii) and iv) electron and ion heat fluxes at $s = l_{\rm c}$ determined by the sheath theory [8, 11].

2.2 Modeling of neutral particle

In order to describe interactions of plasma, hydrogen molecules and atoms, we choose five dominant reactions in the divertor plasma.

(d1) $\mathrm{H_2 + e^- \rightarrow 2H + e^-}$,
(d2) $\mathrm{H_2 + e^- \rightarrow H^+ + H + 2e^-}$,
(cx) $\mathrm{H + H^+ \rightarrow H^+ + H}$,
(iz) $\mathrm{H + e^- \rightarrow H^+ + 2e^-}$,
(rc) $\mathrm{H^+ + 2e^- \rightarrow H + e^-}$.

The fist and second reactions represent the dissociation of hydrogen molecule to atoms. The reaction (d2) consists of two reaction, $\mathrm{H_2 + e^- \rightarrow H_2^+ + 2e^-}$ and $\mathrm{H_2^+ + e^- \rightarrow H^+ + H + e^-}$, but the dissociation rate of $\mathrm{H_2^+}$ is relatively high and the particle speed of $\mathrm{H_2}$ is slow. Thus these two reactions are regarded as one reaction in this work. The last three reactions, (cx), (iz) and (rc), represent charge exchange, ionization and recombination, respectively. The rate coefficient of these reactions [12, 13] are denoted by $\langle\sigma_{\rm d1}v\rangle$, $\langle\sigma_{\rm d2}v\rangle$, $\langle\sigma_{\rm cx}v\rangle$, $\langle\sigma_{\rm iz}v\rangle$ and $\langle\sigma_{\rm rc}v\rangle$, respectively.

There are several types of expressions to obtain the neutral profiles; Monte Carlo simulation, kinetic equation, fluid equation and diffusion equation. Since the mean-free-path (MFP) of hydrogen atom, e.g. approximately 2 [m] for a typical neutral density 10^{19} [m^{-3}], is comparable to the plasma size and much longer than the neutral decay length [8]. Therefore the diffusion process is negligible in the divertor plasma and also the fluid equation of the neutral gas does not correctly describe the characteristics of the wide range of particle energy such as few eV of dissociation atoms and tens eV of charge exchange atoms. Therefore in this paper, we use simplified kinetic-type equations.

We classify the neutrals into four components; molecules released from the divertor plate, dissociated atoms from the molecules, charge exchange atoms and recombination atoms. The particle speed of each component is treated as a constant; $v_{\rm m}$, $v_{\rm d}$, $v_{\rm cx}$ and $v_{\rm rc}$, respectively. The density of each component is denoted by $n_{\rm m}$, $n_{\rm d}^{\pm}$, $n_{\rm cx}^{\pm}$ and $n_{\rm rc}^{\pm}$, respectively. The superscript '±' corresponds to two components with opposite direction, i.e. positive and negative velocity on s-coordinate. They have each characteristic temperature, or energy, determined from their sources. The molecule temperature $T_{\rm m}$ is same as that of the divertor plate. The temperature of dissociation atoms is determined from the Frank-Condon dissociation energy, i.e. $T_{\rm d} \sim 2.5[eV]$. The temperatures of charge exchange and recombination atoms, $T_{\rm cx}$ and $T_{\rm rc}$, are determined from the averages energy of the generated atoms by each processes over $s = 0$ to $l_{\rm c}$. The velocity of each component are calculated from corresponding temperature; $v_{\rm m} = \sqrt{T_{\rm m}/\pi m_{\rm i}}/\cos\varphi$, $v_{\rm d} = \sqrt{2T_{\rm d}/\pi m_{\rm i}}$, $v_{\rm cx} = \sqrt{2T_{\rm rc}/\pi m_{\rm i}}$ and $v_{\rm rc} = \sqrt{2T_{\rm cx}/\pi m_{\rm i}}$. The angle of the magnetic field measured from the surface normal on the divertor plate was denoted by φ and used to obtain the equivalent velocity of molecules. This conversion is due to the existence of the difference between the directions of plasma and neutral flows.

The particle conservation equations of neutrals are given by

$$-v_m\frac{dn_{\rm m}}{ds} = \left(\langle\sigma_{\rm d1}v\rangle + \langle\sigma_{\rm d2}v\rangle\right)n_{\rm m}n, \quad (6)$$

$$\pm v_{\rm d}\frac{dn_{\rm d}^{\pm}}{ds} = \left(2\langle\sigma_{\rm d1}v\rangle + \langle\sigma_{\rm d2}v\rangle\right)n_{\rm m}n - \left(\langle\sigma_{\rm iz}v\rangle + \langle\sigma_{\rm cx}v\rangle\right)n_{\rm d}^{\pm}n, \quad (7)$$

$$\pm v_{\rm H_{cx}}\frac{dn_{\rm cx}^{\pm}}{ds} = (1-r_{\rm pl})\frac{v_{\rm cx}\pm v}{2v_{\rm cx}}\langle\sigma_{\rm cx}v\rangle n_{\rm a}n - \left(\langle\sigma_{\rm iz}v\rangle + \langle\sigma_{\rm cx}v\rangle\right)n_{\rm cx}^{\pm}n, \quad (8)$$

$$\pm v_{\rm rc}\frac{dn^{\pm}_{\rm rc}}{ds} = (1-r_{\rm pl})\frac{v_{\rm rc}\pm v}{2v_{\rm rc}}\langle\sigma_{\rm rc}v\rangle n^2 - (\langle\sigma_{\rm iz}v\rangle + \langle\sigma_{\rm cx}v\rangle)\, n^{\pm}_{\rm rc} n, \quad (9)$$

where the total density of hydrogen atoms were denoted by $n_{\rm a} \equiv n^+_{\rm d} + n^-_{\rm d} + n^+_{\rm cx} + n^-_{\rm cx} + n^+_{\rm rc} + n^-_{\rm rc}$. Since the source of the hydrogen is the molecules released from the divertor plate, we use the boundary condition, $n_{\rm m1}v_{\rm m} = n_1 v_1/2$. The particle loss of generated hydrogen atoms was introduced as a constant ratio $r_{\rm pl}$ in Eqs. (8) and (9). We note that each equations, (7) – (9), consists of two equations for positive and negative velocities. The coefficients of the first terms in the right-hand side of Eqs. (8) and (9), $(v_{\rm cx} \pm v)/2v_{\rm cx}$ and $(v_{\rm rc} \pm v)/2v_{\rm rc}$, represent the momentum conservation in the charge exchange hydrogen atoms and ions. In order to conserve the total energy when $r_{\rm pl} = 0$, the temperature $T_{\rm cx}$ and $T_{\rm rc}$ are calculated as

$$T_{\rm cx} = \frac{\int_0^{l_{\rm c}} \left(T_{\rm i} + m_{\rm i}v^2/3\right)\langle\sigma_{\rm cx}v\rangle n_{\rm a} n\, ds}{\int_0^{l_{\rm c}}\langle\sigma_{\rm cx}v\rangle n_{\rm a} n\, ds}, \quad (10)$$

$$T_{\rm rc} = \frac{\int_0^{l_{\rm c}} \left(T_{\rm i} + m_{\rm i}v^2/3\right)\langle\sigma_{\rm rc}v\rangle n^2\, ds}{\int_0^{l_{\rm c}}\langle\sigma_{\rm rc}v\rangle n^2\, ds}. \quad (11)$$

The source terms in Eqs. (1) – (4) are given by

$$S_{\rm n} = \langle\sigma_{\rm d2}v\rangle n_{\rm m} n_{\rm e} + \langle\sigma_{\rm iz}v\rangle n_{\rm a} n_{\rm e} - \langle\sigma_{\rm rc}v\rangle n_{\rm i} n_{\rm e}, \quad (12)$$

$$S_{\rm p} = m_{\rm i}\langle\sigma_{\rm cx}v\rangle n_{\rm i}\left[\left(n^+_{\rm d} - n^-_{\rm d}\right)v_{\rm d} + \left(n^+_{\rm cx} - n^-_{\rm cx}\right)v_{\rm cx} + \left(n^+_{\rm rc} - n^-_{\rm rc}\right)v_{\rm rc} - n_{\rm a}v\right], \quad (13)$$

$$S_{\rm Ee} = -25e\langle\sigma_{\rm iz}v\rangle n_{\rm a} n, \quad (14)$$

$$S_{\rm Ei} = \frac{3}{2}\left(\langle\sigma_{\rm iz}v\rangle n_{\rm e} + \langle\sigma_{\rm cx}v\rangle n_{\rm i}\right)\left[\left(n^+_{\rm d} + n^-_{\rm d}\right)T_{\rm d} + \left(n^+_{\rm cx} + n^-_{\rm cx}\right)T_{\rm cx} + \left(n^+_{\rm rc} + n^-_{\rm rc}\right)T_{\rm rc}\right] + 4.3e\langle\sigma_{\rm d2}v\rangle n_{\rm e} n_{\rm m} - \langle\sigma_{\rm cx}v\rangle n_{\rm s} n_{\rm i}\left(\frac{3}{2}T_{\rm i} + \frac{1}{2}m_{\rm i}v^2\right). \quad (15)$$

3 Results and discussions

We modified the numerical code in Ref. [8] to solve the plasma equations (1) – (5) and the neutral equations (6) – (9) self-consistently. The plasma equations and neutral equations with negative velocity are integrated from the wall boundary, $s = l_{\rm c}$, and the neutral equations with positive velocity are integrated from the upstream boundary, $s = 0$. The integrals are carried out numerically by the fourth order Runge-Kutta method and the step width is changed adoptively. Since the plasma profiles and neutral profiles depend on each other, we obtain solutions by solving plasma and neutral equations iteratively. The total calculation time including the iterations is less than one second on an ordinary PC. Although the time is longer than that of the previous code [8], it is still reasonable for the integrated simulation in the future plan.

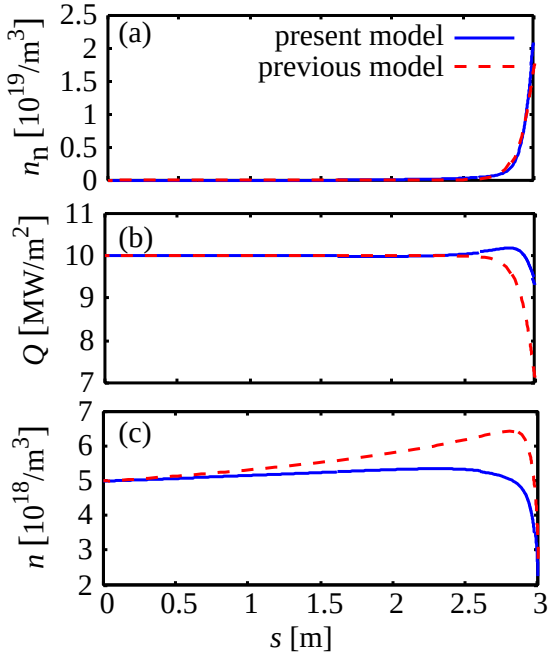

Fig. 1 (a) neutral density, (b) heat flux and (c) plasma density profiles obtained from the previous and present models.

Comparisons of the solutions between present and previous models are shown in Fig. 1. The plasma density and electron and ion heat fluxes at $s = 0$ were chosen as $n_0 = 5 \times 10^{18}$ [m^{-3}], $Q_{\rm e} = Q_{\rm i} = 5$ [MW/m^2]. Temperature of the hydrogen molecules, angle of the magnetic field, particle loss ratio and impurity ratio were $T_{\rm m} = 600$ [K], $\varphi = 80°$, $r_{\rm pl} = 0.2$ and $r_{\rm imp} = 3\%$, respectively. The global recycling coefficient was calculated as 84% from the particle fluxes at $s = 0$ and $l_{\rm c}$. The density profiles of neutrals, $n_{\rm n} = n_{\rm a} + n_{\rm m}$, in Fig. 1(a) were similar each other in this case. The heat flux Q of the previous model in Fig. 1(b), however, had lower value than that of the present one near the divertor plate. The reason of the difference is due to the overestimate of the energy loss by charge exchange in the previous one. A small peak in front of the wall was observed in the Q profile of the present model. It is caused by the interaction of the ion and neutral energy. High speed neutrals are generated through the charge exchange processes and their energy are transported by the neutral flow. The neutrals remaining in the plasma region are ionized and their energy returns to the plasma. Therefore the small peak represents energy transport by neutrals from the vicinity of the wall to $s \sim 2.7$ [m]. The overestimate of the plasma density in Fig. 1(c) is also caused by the overestimate of the energy loss, or underestimate of the ion temperature.

The heat fluxes at the divertor plate, $s = l_{\rm c}$, are shown as functions of the plasma density at $s = 0$ in Fig. 2(a). The electron, ion and total heat fluxes were denoted by $Q_{\rm e1}$, $Q_{\rm i1}$ and Q_1, respectively. The input heat flux is fixed to $Q_{\rm e0} = Q_{\rm i0} = 5$ [MW/m^2]. When the density is rela-

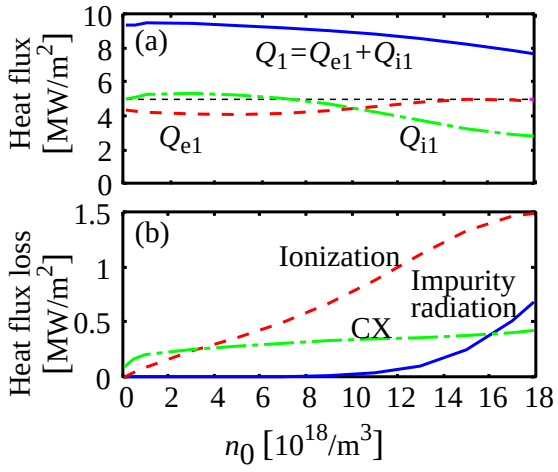

Fig. 2 (a) heat flux at the divertor plate and (b) heat flux loss as functions of plasma density at upstream boundary n_0. Electron, ion and total heat fluxes were denoted by Q, Q_e and Q_i.

tively low, e.g. $n_0 < 10^{19}$ [m^{-3}], almost all heat flux coming from the upstream boundary deposits on the divertor plate, while in the high recycling regime the heat flux decreases and especially the ion heat flux becomes half. The contributions of three main energy sinks to the heat flux are compared in Fig. 2(b). The largest energy loss is caused by radiation due to the electron impact ionization. The loss caused by ionization and impurity radiation increases in high recycling regime because the electron temperature decrease to about 10 [eV], while the charge exchange loss does not change. From above discussions we can identify the energy transfer channels. In the low recycling regime, $n_0 \sim 5 \times 10^{18}$ [m^{-3}], electron and ion energies are lost by ionization loss and charge exchange loss, respectively. The each amount of the loss is comparable and much smaller than the total heat flux coming from the upstream plasma. In the high recycling regime, $n_0 > 1 \times 10^{19}$ [m^{-3}], ionization and impurity losses increases and the plasma energy is lost through the electon channel mainly. The impurity cooling increases more rapidly than ionization for $n_0 > 1.5 \times 10^{19}$ [m^{-3}].

4 Conclusions

A fluid model of LHD divertor plasma and a neutral model were presented. The atomic processes such as dissociation and ionization of hydrogen molecules and atoms were included. We developed a numerical code which has boundary conditions relevant to code connections at the both end of the calculation region, i.e. $s = 0$ and l_c. The self-consistent solutions were obtained by iterative calculations of the plasma and neutral equations. The calculation time is less than one second and it is reasonably short for integrated simulation of future studies.

Comparisons of heat flux, neutral and plasma density profiles between the previous [8] and present models were carried out. Although the deviation of the neutral density was negligibly small, the heat flux and plasma density profiles changed significantly. By treating the interaction of energy between plasma and neutrals directly, the amount of energy loss due to the energetic neutral atoms are included correctly in the model, and thus the overestimate of the energy loss is improved.

The dependence of the heat flux on the plasma density were studied by using the code. In the low density case, the plasma loses its energy by ionization and charge exchange, but effect of the loss on the heat flux decrease is small. On the other hand in the high density, or high recycling case, the ionization loss and impurity cooling becomes large and the heat flux decreases by 20% when the plasma density at the upstream boundary is 1.8×10^{19} [m^{-3}]. We confirmed that the ion energy is transfered to electron and it is lost by ionization and impurity radiation.

In the paper, we employed constant impurity ratio. The dynamics of impurities is important to obtain the impurity profiles and to elucidate the role of the divertor plasma on the core plasma. Implementation of a fluid impurity model and the application of the model to the integrated simulation will be future issues.

Acknowledgments

The contribution of the last author was carried out under the European Fusion Development agreement, supported by the European Communities. The views and opinions expressed herein do not necessarily reflect those of the European Commission.

[1] N. Oyabu *et al.*, Nucl. Fusion, **34**, 387 (1994)
[2] M. Kobayashi *et al.*, J. Nucl. Mater., **363–365**, 294 (2007)
[3] A. Kirschner *et al.*, Nuclear Fusion, **40**, 989 (2000)
[4] P. C. Stangeby and J. D. Elder, J. Nucl. Mater., **196-198**, 258 (1992)
[5] K. Shimizu *et al.*, J. Nucl. Mater., **196-198** 476 (1992)
[6] Rajiv Goswami *et al.*, Phys. Plasmas, **8**, 857 (2001)
[7] Deok-Kyu Kim and Sanh Hee Hong, Phys. Plasmas, **12**, 062504 (2005)
[8] G. Kawamura, Y. Tomita, M. Kobayashi and D. Tskhakaya, *"1D fluid model of plasma profiles in the LHD divertor leg"*, to be published in J. Plasma Fusion Res. Ser.
[9] S. I. Braginskii, Rev. Plasma Phys., **1**, 205 (1965)
[10] D. Tskhakaya and S. Kuhn, Plasma Phys. Control. Fusion, **47**, A327 (2005)
[11] Peter C. Stangeby, *The Plasma Boundary of Magnetic Fusion Devices*, Institute of Physics Publishing (Bristol and Philadelphia 1999).
[12] R. L. Freeman and E. M. Jones, *Atomic Collision Processes in Plasma Physics Experiments*, Culham Laboratory, Abingdon, England, Report CLM-R 137 (1974).
[13] E. M. Jones, *Atomic Collision Processes in Plasma Physics Experiments*, Culham Laboratory, Abingdon, England, Report CLM-R 175 (1977).